JURNAL KIMIA VALENSI
p-ISSN: 2460-6065; e-ISSN: 2548-3013
Journal homepage: https://journal.uinjkt.ac.id/index.php/valensi
Research Article

A Novel Benzenesulfonylurea-Substituted Pyridazinone Derivative with Antidiabetic Effect as the Peroxisome Proliferator-activated Receptor (PPAR-γ) Agonist

Yuni Fatisa[1,2], Arif Yasthophi[2], Elviyenti[2], Ihsan Ikhtiaruddin[3], Neni Frimayanti[3], Hilwan Yuda Teruna[1], Jasril Jasril[1]*

[1]*Department of Chemistry, Faculty of Mathematic and Natural Sciences, Riau University, Pekanbaru, 28293, Indonesia*
[2]*Department of Chemistry Education, Faculty of Tarbiyah and Keguruan, Universitas Islam Negeri Sultan Syarif Kasim University, Pekanbaru, 28293, Indonesia*
[3]*Department of Pharmacy, Sekolah Tinggi Ilmu Farmasi Riau, Pekanbaru, 28293, Indonesia*

**Email: jasril.k@lecturer.unri.ac.id*

Article Info
Received: Nov 2, 2024
Revised: May 5, 2025
Accepted: May 12, 2025
Online: May 31, 2025

Citation:
Fatisa, Y., Yasthophy, A., Elviyenti., Ikhtiaruddin, I., Frimayanti, N., Teruna, H. Y., & Jasril, J. (2025). A Novel Benzenesulfonylurea-Substituted Pyridazinone Derivative with Antidiabetic Effect as the Peroxisome Proliferator-activated Receptor (PPAR-γ) Agonist. *Jurnal Kimia Valensi*, 11(1), 18-29.

Doi: 10.15408/jkv.v11i1.42187

Abstract

Peroxisome Proliferator-activated Receptor (PPAR-γ) protein is one of the target proteins for insulin sensitivity therapy in Type 2 DM. PPAR-γ has a key role as a nuclear receptor that regulates the expression of several metabolism-related genes. This research aims to synthesize a novel benzenesulfonylurea-substituted pyridazinone derivative, namely (E)-N'-(1-(4-(3-(4-methoxyphenyl)-6-oxopyridazin-1(6*H*)-yl)phenyl)ethylidene)-4-methylbenzenesulfonohydrazide (**8**) and predicted it activity as the PPAR-γ agonist using a molecular docking approach and ADMET profiles. The compound **8** was obtained through a Schiff base condensation reaction between compound **6**, p-tosyl hydrazine, and a glacial acetic acid catalyst using monowave. The purity of the compound was determined by TLC test, and melting point measurement. The structure was confirmed through FTIR, 1H-NMR, C-NMR and HRMS analysis. Molecular docking studies were carried out on the crystal structure of the human PPAR-γ Ligand Binding Domain target protein in complex with the α-aryloxyphenyl acetic acid agonist (PDB ID 1ZEO). The results of the docking show that compound **8** has a lower binding free energy than rosiglitazone (positive control) with a free energy value (S score) = -13.513 kcal/mol and -8.3089 kcal/mol, respectively. Compound **8** can form two hydrogen bonds with residues His323 and Ser289, π-π interactions with Phe363 and π-H interactions with Cys285. The interactions are similar to the interaction between the native ligand agonists α-aryloxyphenyl acetic acid and rosiglitazone with the target protein. Furthermore, compound **8** is predicted to have a moderate ADME profile. The results support that compound **8** can be developed as a PPAR-γ agonist candidate for the antidiabetic therapeutic agent.

Keywords: ADMET, schiff base condensation, molecular docking, PPAR-γ agonist

1. INTRODUCTION

Diabetes mellitus is a metabolic disease that has become common in developed and developing countries. Around 85-90% of cases of DM are type 2 diabetes mellitus (T2DM). The pathogenesis of T2DM is caused by the failure of pancreatic β-cells to produce insulin and insulin resistance, which is characterized by hyperglycemia. In 2021, the number of adult diabetes patients aged 20-79 years was estimated at 537 million. This number is predicted to increase to 783 million by 2045 [1]. Diabetes patients can develop complications into various diseases such as cardiovascular disease, stroke, coronary heart disease, retinopathy, cataracts, and kidney failure, etc [2,3].

The metabolic disease is multifactorial causing hyperglycemia, which is associated with various receptor activities and enzymes involved in glucose metabolism. Target receptors such as PPAR, GLP-1R, melatonin, GPCRs, GPER, and others are current targets that have become the focus of developing new

therapies for metabolic disorder [4–6]. Peroxisome Proliferator-Activated Receptor Gamma (PPAR-γ) receptor one of the important for insuline sensitivity therapy. Low or abnormal expression of nuclear receptors can cause impaired insulin action, which is one of the symptoms of Type 2 Diabetes Mellitus [7]. PPAR-γ is a multi-domain nuclear transcription factor that resides in the cytoplasm of cells. After binding to activating ligands (small molecules), PPAR-γ will translocate to the nucleus to bind to specific DNA segments and regulate gene expression. Genes activated by PPAR-γ are associated with adipocyte or fat cell differentiation and lipid storage/release, glucose metabolism pathways, and anti-inflammation [8].

Both natural and synthetic endogenous ligands have been developed as PPAR-γ agonists to improve insulin resistance. One of the synthetic agonist ligands commonly used for this is the thiazolidinedione (TZD) group. However, some of these synthetic ligands were recalled from the market due to their toxicity. Currently, rosiglitazone and troglitazone are approved by the FDA for use as therapy. However, over a long period, the use of these drugs can cause hepatotoxic and cardiovascular side effects [9,10]. Several studies have also developed non-TZD PPAR-G agonists, which have safer and more efficacious properties [11,12]. However, this is still being researched as it enters various phases of clinical trials. So the need for PPAR α/γ and PPAR δ/γ agonist ligands it is a challenge to develop.

One group of six-ring heterocyclic compounds that is interesting to be developed as an antidiabetic agent is the pyridazinone derivatives. The literature reveals that they exhibit various pharmacophore effects, such as anti-imflammatory [13], antioxidant [14], COX-2 inhibitor [15,16], antimicrobials [17], and selective inhibitors of BuChE [18]. As antidiabetics, some pyridazinone-derived compounds (**Figure 1**) show antihyperglycemic, inhibitor α-glucosidase and inhibitor aldose reductase [19–24] . Therefore, this group of compounds has the potential to be developed as antidiabetic materials.

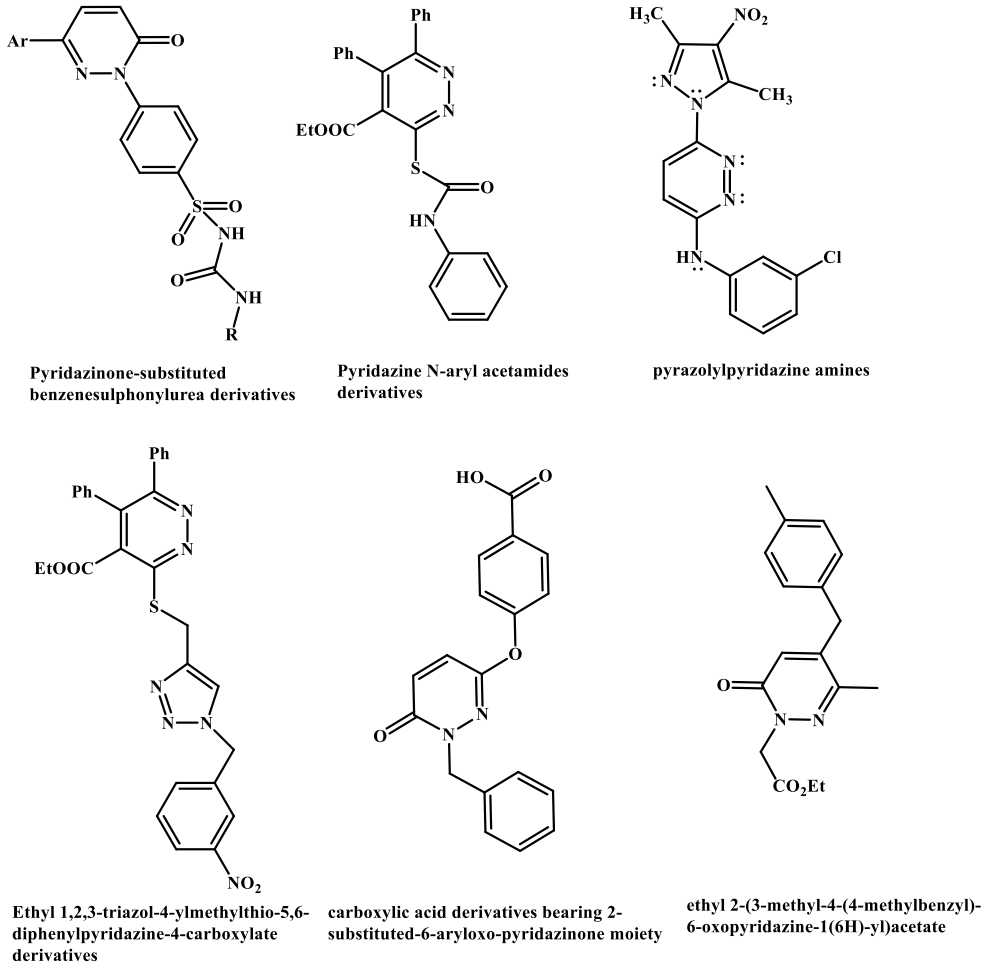

Figure 1. Antidiabetic activity of pyridazinone-derived compounds [19,21–25]

Kharbanda et al. [26] reported that pyrazoline compounds containing a sulfonylurea benzene ring have the potential as PPAR-γ agonists and anticancers using in vivo tests. These results were confirmed

through molecular docking studies. Yaseen et. al [19] have found that aryl pyridazinone-substituted benzenesulphonylurea derivatives possess significant dual action as antihyperglycaemic and aldose reductase inhibition based on docking and in vitro study. This research carried out a novel benzene sulphonylurea-substituted pyridazinone derivative (8) through three reaction stages. The new compound **8** is a hybrid hidrazon-sulphonylurea-substituted pyridazinone, which has never been synthesized before and has never been reported. Benzenesulphonylurea substituent bound to pyridazinone was selected based on studies of antidiabetic activities above. In addition, sulfonylurea derivatives are market drugs that can increase insulin secretion in pancreatic β-cells, such as glibenclamide, glicazide, and others. So, the contribution of benzenesulfonylurea substituent bound to pyridazinone to activity was investigated and aimed at finding the precursor molecule for bioactivity. Furthermore, the antidiabetic activity of the novel target as a PPAR-γ protein agonist (PDB ID 1ZEO) was evaluated using the Molecular Operating Environment (MOE) 2020.0102 program. This study was carried out to predict the mechanism of ligand-receptor action in more detail. Data analysis involves binding free energy and RMSD values, and the best pose of compounds with PPAR-γ residues in the active site. Meanwhile, the ADMET profile properties (adsorption, distribution, metabolism, excretion, and toxicity) are predicted to obtain drug candidates bioavailability and safety characteristics of using an online database.

2. RESEARCH METHODS

Instruments and Materials

All reagents were used without further purification: 4-methoxy acetophenone (Sigma-Aldrich), Hydrazine (Sigma-Aldrich), glyoxylic acid (Sigma-Aldrich), 4-fluoro acetophenone (Sigma-Aldrich), glacial acetic acid (Merck), 4-Methylbenzenesulfonhydrazide (Merck), potassium carbonate (Merck), and organic solvents.

The synthesis reaction was carried out using a sealed-vessel reactor Mono wave 50 (Anton-Paar, Graz, Austria). The melting point was determined on a Fisher-Johns apparatus (Fisher Scientific, Waltham, MA, USA) (uncorr). Thin Layer Chromatography (TLC) analysis was carried out using GF254 (Merck Millipore, Darmstadt, Germany) under a UV lamp 254/365 nm (Cole-Elmer®, Vernon Hills, IL, USA). The FT-IR spectrum was recorded in KBr powder on a Shimadzu® FT-IR Prestige-21 spectrophotometer (Shimadzu Corporation, Kyoto, Japan), and the Mass spectrum was measured using a Waters Xevo QTOFMS instrument (Waters, Milford, MA, USA). The 1H-NMR spectra were recorded on an Agilent® (Agilent Technologies, Santa Clara, CA, USA) at 500 and 125 MHz, respectively. The molecular docking studies was carried out using the MOE 2020.0102 software package and Discovery Studio Visualizer (DSV) 2019 software.

Synthesis of 6-(4-methoxy phenyl-pyridazine)-3(2H)-one (4).

Synthesis of 6-(4-methoxy phenyl-pyridazine)-3(2H)-one (**4**) was prepared by modifying the procedure proposed by [27]. A mixture of glyoxylic acid (3 mmol), 4-methoxy acetophenone (3 mmol), and glacial acetic acid (3 mL) was reacted in monowave at 120 ^{0}C, and after 3 hours of reaction, followed by the addition of hydrazine monohydrate (3 mmol) to the reaction mixture for 2 hours. The mixture was neutralized by adding NaOH solution. The precipitate was filtered and washed with cold demineralized (DM) water (25 mL), then dried at room temperature. After that, the product was washed with hot n-hexane (10 mL) and dried at room temperature.

Molecular formula $C_{11}H_{10}N_2O_2$, brown solid (81.84 % yield). m.p. 148-149 ^{0}C. FT-IR spectrum (KBr) $\bar{U}$ (cm^{-1}): 3201 (N-H amine), 2908 (C-H sp^3), 1655 (C=O), 1593 (C=N). ^{1}H-NMR (500 MHz, $CDCl_3$) δ (ppm): 11.55 (s, 1H), 7.74 (d, *J* = 8.5 Hz, 2H), 7.74 (d, *J* = 10.0 Hz, 1H), 7.06 (d, *J* = 10.0 Hz, 1H), 6.99 (d, *J* = 8.5 Hz, 2H), 3.87 (d, *J* = 1.0 Hz, 3H). HRMS (ESI): m/z 203.0826. $[M + H]^+$ (calcd. for $C_{11}H_{10}N_2O_2$: 203.0821).

Synthesis of 2-(4-acetylphenyl)-6-(4-methoxyphenyl)pyridazine-3(2H)-one (6).

Synthesis of 2-(4-acetylphenyl)-6-(4-methoxyphenyl)pyridazine-3(2H)-one (**6**) was prepared by modifying the procedure proposed by [28]. A mixture of compound **4** (1 mmol), 4-fluoro acetophenone (1.25 mmol), and potassium carbonate (1.5 mmol) in DMSO (4 mL) was reacted in monowave at 100 ^{0}C for 6 hours. Reaction was controlled using TLC with the eluent hexane: ethyl acetate (6:4). The reaction mixture was poured into ice water. The precipitate obtained was filtered, washed with cold demineralized (DM) water (25 mL), and dried at room temperature. After that, the product was washed with hot n-hexane (mL), then dried at room temperature.

Molecular formula $C_{19}H_{16}N_2O_3$, brown solid (24 % yield). m.p. 152-154 ^{0}C. FT-IR spectrum (KBr) $\bar{U}$ (cm^{-1}): 2999 (C-H sp_3), 1676 (C=O), 1518 (C=N). ^{1}H-NMR (500 MHz, $CDCl_3$) δ (ppm): 8.10 (d, *J* = 8.7 Hz, 2H), 7.91 (d, *J* = 8.7 Hz, 2H), 7.79 (d, *J* = 8.9 Hz, 2H), 7.75 (d, *J* = 9.8 Hz, 1H), 7.14 (d, *J* = 9.8 Hz, 1H), 7.00 (d, *J* = 8.9 Hz, 2H), 3.88 (s, 3H), 2.66 (s, 3H). HRMS (ESI): m/z 321.1239 $[M + H]^+$ (calcd. for $C_{19}H_{16}N_2O_3$: 321.1246).

Synthesis of E)-N'-(1-(4-(3-(4-methoxiphenyl)-6-oxopyridazine-1(6H)-yl)phenyl)ethylidene)-4-methylbenzenesulphonohydrazide (8)

Synthesis of compound **8** was carried out according to the literature method [16]. A mixture of compound **6** (1 mmol), p-toluenesulphonylhydrazide (4 mmol), ethanol (5 mL), and glacial acetic acid (3 mL) was heated to 300 watt for 3-10 min using the microwave. Reaction control was carried out using TLC with the eluent hexane: ethyl acetate (4:6). After that, cold DM water (2 mL) was added to the mixture, then the pH of the mixture was neutralized with 6N NaOH solution. The mixture is left in the freezer for 24 hours. The precipitate was filtered and washed with cold demineralized (DM) water (25 mL), then dried at room temperature. After that, the product recrystallized from ethanol.

Molecular formula $C_{26}H_{24}N_4O_4S$, yellow solid (16 % yield). m.p. 147-149 ^{0}C. FT-IR spectrum (KBr) $\tilde{U}$ (cm^{-1}): 3349 (N-H amine), 2811 (C-H sp^3), 1701 (C=O), 1515 (C=N), 1334 (SO_2). ^{1}H-NMR (500 MHz, $CDCl_3$), δ (ppm): 8.09 (s, 1H), 7.92 (d, *J* = 8.0 Hz, 2H), 7.77 (dd, *J* = 13.2, 9.3 Hz, 3H), 7.70 (d, *J* = 8.4 Hz, 2H), 7.62 (d, *J* = 8.3 Hz, 2H), 7.32 (d, *J* = 8.0 Hz, 2H), 7.16 (d, *J* = 9.7 Hz, 1H), 7.00 (d, *J* = 8.9 Hz, 2H), 3.88 (s, 3H), 2.42 (s, 3H), 2.08 (s, 3H). ^{13}C-NMR (126 MHz, $CDCl_3$), δ (ppm): 160.98, 159.39, 151.35, 144.92, 144.21, 142.56, 136.76, 135.38, 131.38, 130.21, 129.61, 128.52, 128.14, 127.47, 126.60, 125.16, 114.41, 55.42, 21.60, 13.26. HRMS (ESI): m/z 488.1415 $[M + H]^+$ (calcd. for $C_{26}H_{24}N_4O_4S$: 488.1416).

Molecular Docking

The crystal structure of Human PPAR-γ (PDB ID 1ZEO with resolution 2.50 Å) ligand binding domain complexed with an alpha-aryloxyphenylacetic acid agonist was retrieved from the protein database (https://www.rcsb.org/). A Molecular docking study was carried out using Molecular Operating Environment 2020.0101 software (MOE, Chemical Computing Group, Inc.). The receptor was prepared using Discovery Studio software in the first preparation stage. The PPAR-γ receptor is composed of two monomer chains (A and B). Chain B is removed, while chain A is retained for the docking process. In the next stage, the receptor was prepared using MOE. Water molecules are removed from the receptor. Protonation and correction of atoms are prepared via the computing menu -> energy minimizing (forcefield CHARM27 and walls centroid x = 13.5143, y= -0.2574, z =16.8463). Next, select the compute menu -> prepare -> quick prepare -> gradient (RMS gradient 0.001 kcal/mol/ Å). The 1ZEO receptor is saved in .pdb format.

All ligands were drawn in ChemOffice v.17. Next, the ligand is copied to the MOE interface. Ligands are prepared via the compute menu-> energy minimize -> forcefield (MMFF94x and gradient 0.001)-> fixed hydrogen-> ok. Ligands are stored in the entry database (MDB).

The prepared receptors are opened via MOE again. Before docking, the active site on the receptor is selected via the compute menu -> site finder -> apply -> select site -> dummy atom. Docking simulation is carried out via the dock menu -> site (dummy) -> ligand (MDB file) -> output (name the file in .mdb format). The method uses placement (Triangle Matcher) and Refinement (Rigid Receptor). The scoring functions used are London dG and GBVI/WSA dG. Next, the best pose is taken as 100/10.

ADMET Profiles

ADME properties were analyzed using preADME (https://preadmet.webservice.bmdrc.org/), which includes blood-brain barrier (BBB), human intestinal absorption (HIA), plasma protein binding (PPP), skin permeability, Caco-2 cell permeability, and MDCK permeability. The AdmetSAR (http://lmmd.ecust.edu.cn/admetsar1/predict/) and Protox II (https://tox-new.charite.de/) are used to predict amest toxicity, hepatotoxicity, skin sensitization, carcinogenicity, acute oral toxicity (LD_{50}), and toxicity classification. Bioavailability properties were estimated based on Lipinski's Rule of Five using the IIT Delhi signature of the Supercomputing Facility for Bioinformatics and Computational Biology (SCFBio) (http://www.scfbio-iitd.res.in/software/drugdesign/lipinski.jsp#anchortag). The standard parameters are molecular weight (500), hydrogen bond donor (5), hydrogen bond acceptor (10), and high lipophilicity (expressed as LogP 5).

3. RESULTS AND DISCUSSION

Chemistry

Synthesis of a novel benzene sulphonylurea substituted pyridazinone derivative, namely E)-N'-(1-(4-(3-(4-methoxyphenyl)-6-oxo pyridazine-1 (6H)-yl)phenyl)ethylidene)-4-methylbenzenesulphonohydrazide (**8**) is carried out through three reaction stages (**Figure 2**). In the first stage, 4-methoxy acetophenone was reacted with glyoxylic acid, hydrazine hydrate, and acetic acid catalyst using monowave with the one-pot method for 6 hours to obtain 6-(4-methoxy phenyl-pyridazine)-3(2*H*)-one (**4**). In previous studies, the pyridazinone synthesis process generally consists of several reaction stages, namely the reaction stage between glyoxylic acid and acetone to produce an intermediate compound (crotonic acid), the extraction stage to obtain a pure crotonic acid, and the last is the reaction of crotonic acid and hydrazine to obtain a pyridazinone ring product [18,29,30]. In this study, the one-

pot method provides the advantage of being more concise, faster, saves solvents, and obtains good yields (81.84%). The basic principle of the mechanism is an aldol condensation reaction, where the acid catalyst (CH_3COOH) takes the H atom from the methyl group to form an enol ion. Next, the active methylene nucleophile attacks the carbonyl group of glyoxylic acid to form an α, β-unsaturated carbonyl crotonic acid intermediate. Then, hydrazine hydrate was directly added into the mixture tube to form the pyridazinone ring to produce **4**.

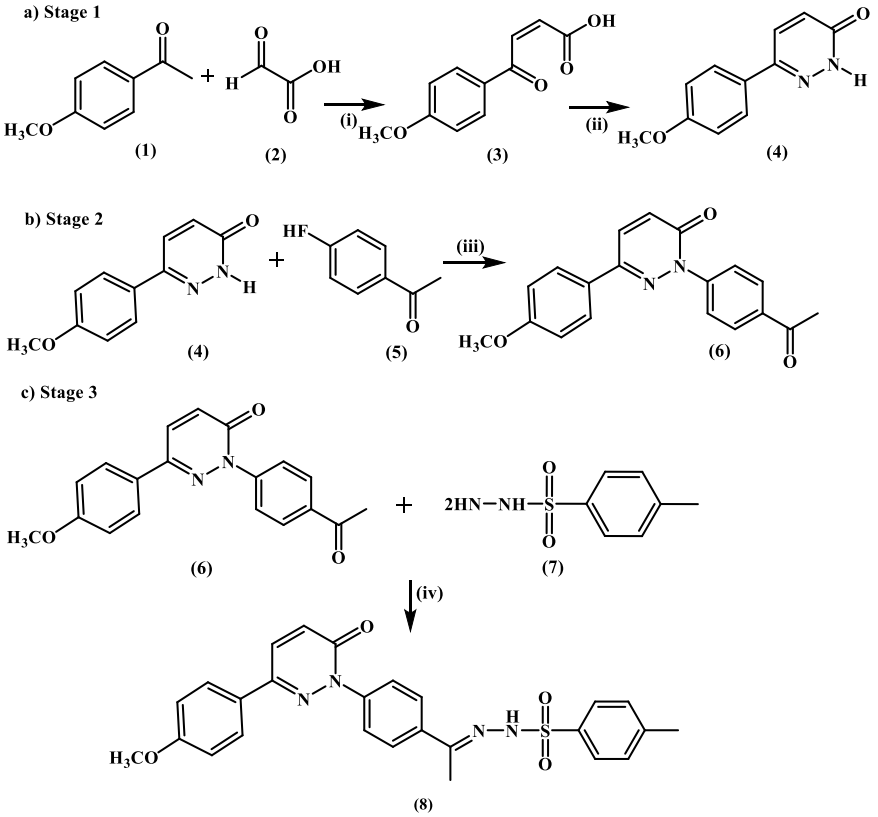

Figure 2. Design concept for the synthesis of novel compound **8**. a) Stage 1: (i) acetic acid glacial, (ii) Hidrazine; b) Stage 2: (iii) K_2CO_3 catalyst; c) Stage 3: etanol/acetic acid glacial

In the second work, compound **4** was reacted with 4-fluoroacetophenone and K_2CO_3 catalyst using monowave at 100 ^{0}C. The substitution reaction mechanism is the base catalyst K_2CO_3 taking the hydrogen atom in the N-H group, thereby increasing the nucleophilic properties of the nitrogen atom. Then, the nitrogen atom attacks the partially positive carbon atom in the C-F bond of the compound 4-fluoroacetophenone. As a result, the F group is released and replaced with compound **4** to produce 2-(4-acetylphenyl)-6-(4-methoxyphenyl)pyridazine-3(2*H*)-one (**6**). In the third stage, *p*-methyl tosylhydrazine was reacted with compound **6** for a novel compound product (**8**). The basic principle of the reaction is the condensation reaction, where nucleophilic amine attacks to the carbonyl group of compound **6** to form an imine (Schiff base) and a water molecule (H_2O) is eliminated [31].

The results of FTIR spectroscopy analysis show a wave number corresponding to the presence of functional groups in compound **6**. A wavenumber of 1676 cm^{-1} indicates the existence of C=O bond stretching vibrations. The wave number of C=N bond stretching, the aliphatic C-H bond stretching, and the aromatic C-H bond stretching are shown at 1518 cm^{-1}, 2999 cm^{-1}, and 3105 cm^{-1}, respectively. IR analysis also shows that there is no wave number for the N-H group because the acetophenone group has substituted it.

The results of the ^{1}H-NMR characterization spectrum (**Figure 3**) show a signal peak that is characteristic of the pyridazinone ring, where the proton signals Hα and Hβ appear at a chemical shift of 7.75 ppm (J= 9.8 Hz) with a doublet orientation and 7.14 ppm (J= 9.7 Hz) with a doublet orientation. Furthermore, the results of this characterization also do not show any proton signal from the N-H group bound to C2, which means that a substitution reaction with fluoroacetophenone has occurred. The presence of protons from two methyl substituents is indicated by two singlet peaks, each in the downfield area of 3.88 ppm and the upfield area of 2.66 ppm. The

protons from methyl attached to the carbonyl carbon are more downfield than the protons of the methoxy group. It means that the electron density around the carbonyl group decreases because the carbonyl carbon attracts more electrons, so the peak signal will appear at a chemical shift that is more deshielding than the chemical shift of the methoxy proton.

The results of FTIR spectroscopy analysis for compound **8** show that there are C=O bond (ketone) stretching vibrations, C-N stretching vibrations, C=N stretching vibrations, aliphatic C-H stretching vibrations at wave numbers 1701 cm^{-1}, 1276 cm^{-1}, 1515 cm^{-1}, and 2811 cm^{-1}, respectively. Furthermore, the wave number 3349 cm^{-1} indicates the stretching vibration of the N-H bond. The SO_2 group is at a wave number of 1334 cm^{-1}.

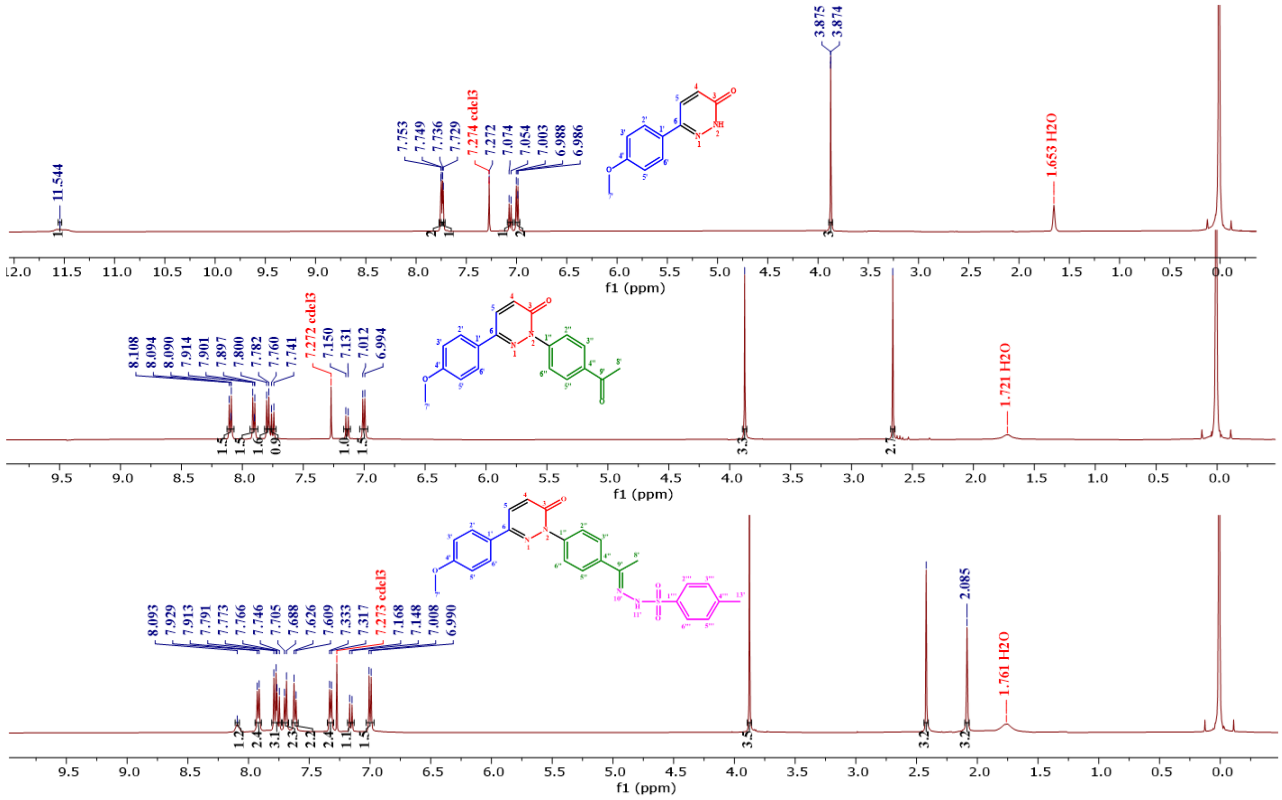

Figure 3. ^{1}H-NMR spectrum of compounds **4**, **6**, **8**

Table 1. ^{1}H-NMR dan ^{13}C-NMR data spectrum of compound **8**

position	δ (ppm) (Multiplisitas, *J*, H)	δC (ppm)	Position	δ (ppm) (Multiplisitas, *J*, H)	δC (ppm)
1	-	-	**1”**	-	126.89
2	-	-	**2”**	7.92 (d, *J* = 8.0 Hz, 2H)	126.61
3	-	161.00	**3”**	7.70 (d, *J* = 8.4 Hz, 2H)	125.17
4	7.16 (d, *J* = 9.7 Hz, 1H)	128.53	**4”**	-	142.58
5	7.77 (dd, *J* = 13.2, 9.3 Hz, 3H)	135.40	**5”**	7.70 (d, *J* = 8.4 Hz, 2H)	125.17
6	-	144.94	**6”**	7.92 (d, *J* = 8.0 Hz, 2H)	126.61
1’	-	131.39	**1’”**	-	136.78
2’	7.77 (dd, *J* = 13.2, 9.3 Hz, 3H)	128.15	**2’”**	7.62 (d, *J* = 8.3 Hz, 2H)	127.48
3’	7.00 (d, *J* = 8.9 Hz, 2H)	114.43	**3’”**	7.32 (d, *J* = 8.0 Hz, 2H)	129.62
4’	-	159.41	**4’”**	-	144.22
5’	7.00 (d, *J* = 8.8 Hz, 2H)	114.43	**5’”**	7.32 (d, *J* = 8.0 Hz, 2H)	129.62
6’	7.77 (dd, *J* = 13.2, 9.3 Hz, 3H)	128.15	**6’”**	7.62 (d, *J* = 8.3 Hz, 2H)	127.48
7’	3.88 (s, 3H)	55.43	**NH11’**	8.09 (s, 1H)	
8’	2.42 (s, 3H)	13.27	**13’**	2.08 (s, 3H)	21.61
9’	-	151.37			
10’	-				

Interpretation of ^{1}H-NMR data for compound **8** also shows proton peaks that are characteristic of pyridazinone derivative compounds, including Hα and Hβ proton signals. The Hα and Hβ proton signals appear at chemical shifts of 7.82-7.71 ppm and 7.13 ppm (J=9.7 Hz) and with a doublet orientation. The

protons in Hα appear as multiplet peaks due to overlapping with the peaks of the 2'"/3'", 5'"/6'" protons. The results of this characterization show that protons from the NH group at 7.33 ppm (dd, J = 13.1, 7.9 Hz, 3H) overlap with the peaks of the 2' and 6' protons. A single peak indicates the presence of three methyl substituents, each in the downfield area of 3.88 ppm, 2.44 ppm, and 2.16 ppm. The binding position of each group in the para position with three aromatic benzene rings is indi-cated by the presence of a symmetrical proton peak of 9 protons (3'/5' and 2'/6'; 3"/5" and 2"/6"; 3 '"/ 5'" and 2'"/ 6'"). The similar chemical environment of 3'/5' and 3"/5" causes proton peaks to appear at 7.33 (dd, J = 13.1, 7.9 Hz, 3H) and δ 7.92 (d, J = 8.2 Hz, 2H), respectively. Likewise, the protons from 2'/6' and 2"/6" have similar chemical environments, so the proton peaks appear at 7.33 (dd, J = 13.1, 7.9 Hz, 3H) and 7.57 (d, J = 13.5 Hz, 1H).

The ^{13}C-NMR spectrum of compound **8** (**Figure 4**) shows a signal of the 8'" carbon atom at δC 151.35 ppm. These changes confirm that a hydrazone formation reaction (C=N) has occurred. ^{1}H-NMR and ^{13}C-NMR spectra of the compound is depicted in **Table 1.**

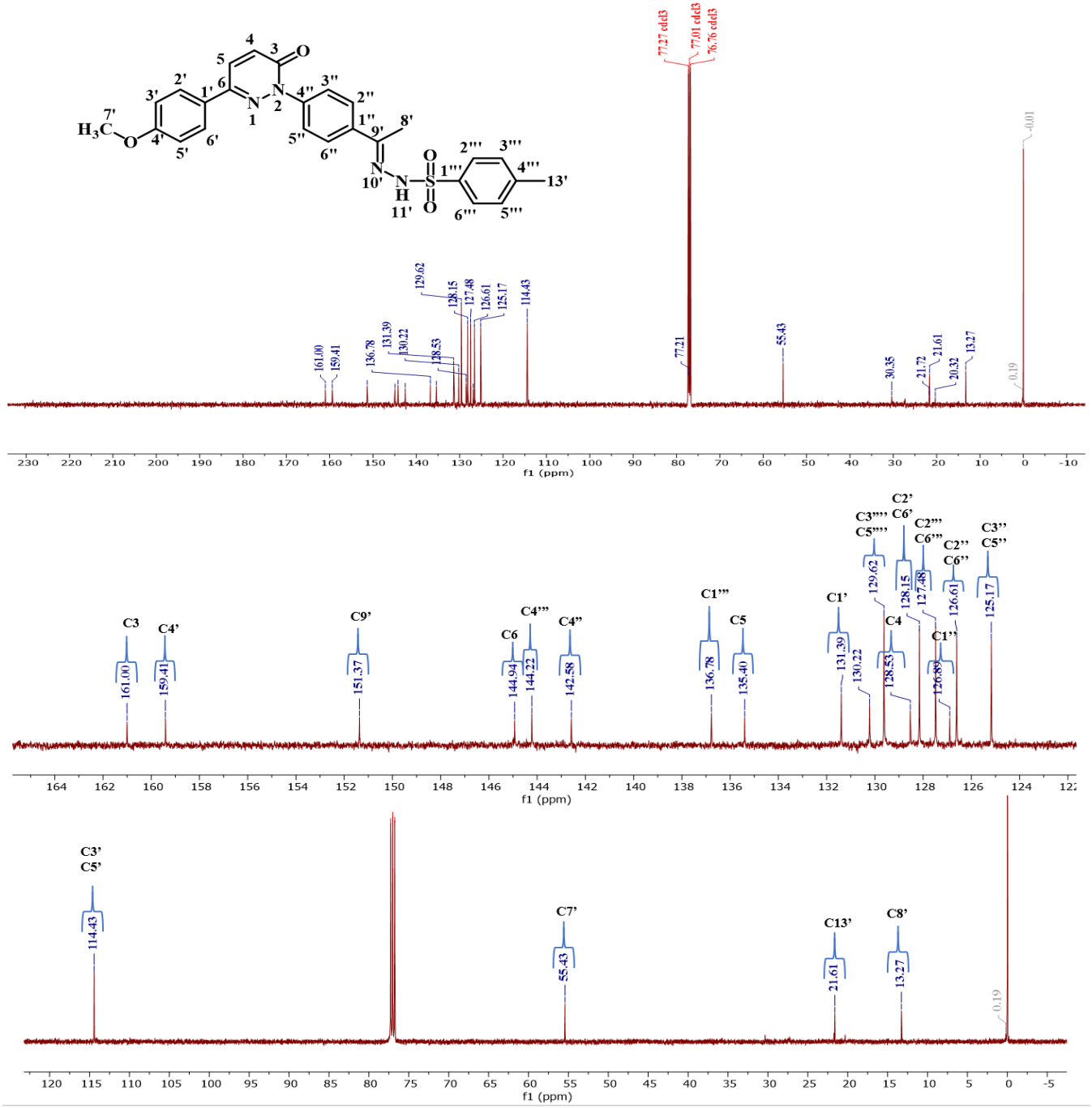

Figure 4. ^{13}C-NMR spectrum of compound **8**

Molecular Docking Studies

The molecular docking studies investigated the intermolecular interaction between the ligand and the receptor. The docking complex was selected based on two criteria: the highest docking score of ligand pose and its oriented into the active site similar to the control orientation.

The PPAR-γ receptor in 1ZEO comprises two monomer chains (A and B). Chain B is removed because Chain B is part of the DNA-inding domain (DBD). Chain A, the ligand binding domain (LBD) is retained for use in the docking process. This refers to Guo Q. Shi's [32], PPARγ-LDB is selected where an alpha-aryloxyphenylacetic acid agonist cocrystallizes with PPARγ-LDB (residues Gln203 to Tyr477), forming a binary complex without coactivator/corepressor peptides.

In the next stage, the PPAR-γ receptor is prepared for docking purposes. In the receptor preparation process, the CHARMM27 force field parameterized for all atom proteins, DNA, and RNA force field is selected [33]. For ligand preparation, the MMFF94x force field is selected. It describes the equations to calculate the potential energy and the parameters for small organic molecules in medicinal chemistry [34].

The co-crystal ligand was redocked on the PPAR-γ receptor using the parameters available in the MOE software to obtain a valid docking method. The docking results show that the redocked native alpha-aryloxyphenylacetic acid occupies the same binding pocket as the native ligand with binding free energy = -13.8151 kkal/mol and RMSD = 0.4983 Å. This value indicates that the co-crystal ligand redocked conformation is similar to the co-crytal ligand. This result is also supported by the superimposition pose formed between the best conformation pose of the redocked native ligand and the native ligand. So, this docking method can be used to dock the test ligand. This interaction and superimposition is shown in **Figure 5**.

Based on the study results (**Table 2**), compound **8** represents the ligand pose with binding free energy (S) = -13.513 kCal/mol and RMSD value < 2 (RMSD = 1.8274). Meanwhile, a positive control PPARG agonist, rosiglitazone, has binding free energy (S) = -8.3089 kCal/mol and RMSD = 1.2608. The more negative the S value, the higher the compound's affinity. These results indicate that compound **8** has a greater affinity than rosiglitazone.

In this study, rosiglitazone shows hydrogen bond interactions with His449 and Tyr473. This result is aligns research by Nazreen *et al.* [35] where rosiglitazone can form three hydrogen bonds with His449, Tyr473, and Cys285. Meanwhile, according to Shi *et al* [32], the co-crystal ligand Alpha-Aryloxyphenylacetic Acid binds to the PPAR-γ receptor to form a hydrogen bond interaction between its carbonyl group and Ser289, His323, His449, and Tyr473. The isoxazolone ring moiety forms hydrophobic interactions with Ile281, Phe282, Cys285, Phe363, and Met364 in the hydrophobic pocket of PPAR-γ.

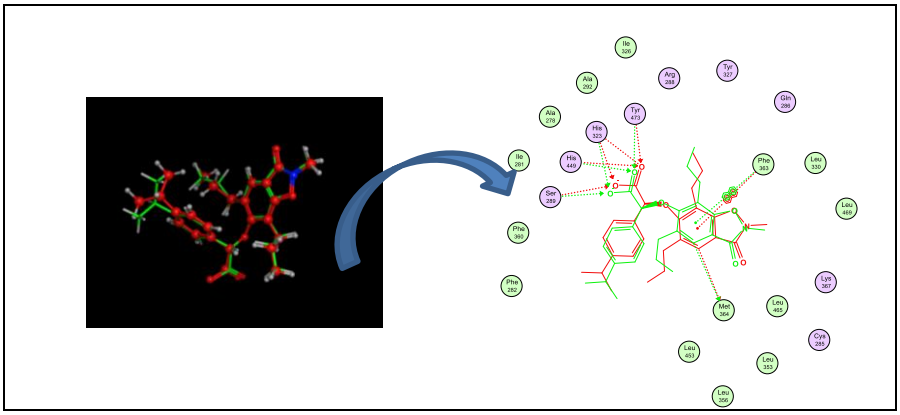

Figure 5. Interaction and superimposition of co-crystal alpha-aryloxyphenylacetic acid ligand (red) with redocked co-crystal alpha-aryloxyphenylacetic acid ligand alpha-aryloxyphenylacetic acid (green) with residues in the active site of the PPAR-γ receptor (1ZEO)

Table 2. Free binding energy value and interaction of ligands with the active site of the PPARG

Compounds	ΔG (kcal/mol)	RMSD	Hydrogen Bond	Hydrophobic interaction
Compound **8**	-13.51	1.83	His323, Ser289	Phe363, Cys285
Rosiglitazone	-8.31	1.21	His449, Tyr473	Ile34, Phe282
α-Aryloxyphenylacetic Acid	-13.81	0.49	His449, Tyr473, His323, His323, er289	Phe363, Met364

Based on the analysis of previous research, compound **8** forms interactions similar to the native ligand and rosiglitazone. It interacts with two hydrogen bond interactions with His323 and ser289, and hydrophobic bonds with Phe363 (π-π interaction) and Cys285 (π-H interaction). Based on the results, the S value of compound **8** is smaller than that of the positive control rosiglitazone. On the other hand, the test compound has similar interactions with rosiglitazone. For these two reasons, it can be concluded that compound **8** is predicted more active as a PPAR-γ agonist than rosiglitazone. This opens up opportunities for developing compound **8** as an antidiabetic candidate.Visualization of the interaction of compound **8** and Rosiglitazone on PPARG can be seen in **Figure 6**.

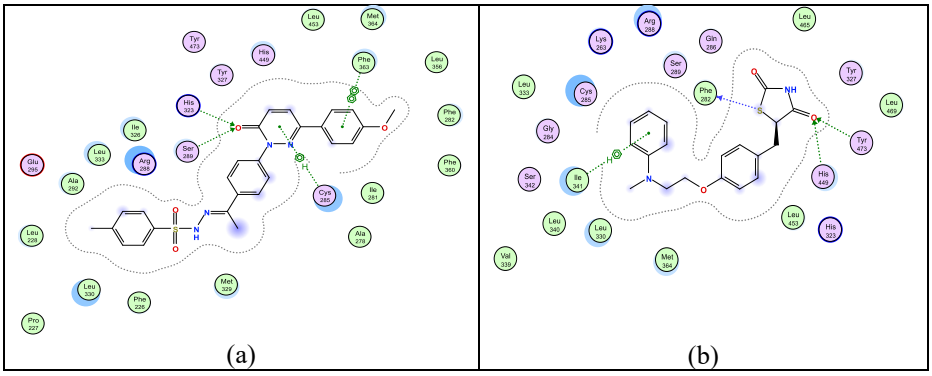

Figure 6. Interaction of ligand poses with residues of the PPARG (1ZEO) receptor: (a) Compound **8**; (b) Rosiglitazone

Table 3. ADMET profiles of compound **8**

ADMET Pofiles	Values
Lipinski's rule of five	
Molecular Weight ≤ 500	488
Hydrogen Bond Donor ≤ 5	0
Hydrogen Bond Acceptor ≤10	8
LogP ≤ 5	5
ADME	
Penetration of Blood Brain Barriers (BBB) *	0.014
Human Intestinal Absorption (HIA) (%) **	96.527
Plasma Protein Binding (PPP) (%) ***	100
Caco2 cell permeability (nm/sec)****	16.041
Skin permeability	-2.3054
MDCK permeability	0.049
Toxicity	
Ames Toxicity	no
hepatoxicity	yes
skin sensitization	no
Carcinogenicity	no
Rat acute oral toxicity (LD50) (mg/kg)	1000
Class*****	4

*BBB: > 2.0 (high absorption to CNS); 2.0 ~ 0.1 (middle absorption to CNS CNS); < 0.1(low absorption to CNS CNS)
**HIA: 0 ~ 20 % (poorly absorbed compounds); 20~70 % (moderately absorbed compounds); 70 ~ 100 (well absorbed compounds)
***PPP: > 90 % (chemicals strongly bound); < 90 % (chemicals weakly bound)
****Caco2 cell permeability; < 4 (low permeability); 4 ~ 70 (middle permeability); > 70 (High permeability)
***** Class I: LD50 ≤ 5 (fatal if swallowed); Class II: 5 < LD50 ≤ 50 (fatal if swallowed); Class III: 50 < LD50 ≤ 300 (toxic if swallowed); Class IV: 300 < LD50 ≤ 2000 (harmful if swallowed); Class V: 2000 < LD50 ≤ 5000 (may be harmful if swallowed); Class VI: LD50 > 5000 (non-toxic)

ADMET Profiles

Lipinski's rule aims to evaluate the pharmacological activity of a chemical com-pound when administered orally to humans. If a chemical compound meets the Lipinski rule criteria, then the compound is considered to have good absorption and permeability potential in the body [36]. Based on **Table 2**, compound **8** meets Lipinski's criteria, because it has a molecular weight of 488, a log P value of 5, several H-bond donors of 0, and several H-bond acceptors of 8. It can be predicted that the target compound is easily absorbed and has good permeability.

ADMET profiles of compound **8** can be seen in **Table 3**.The pharmacokinetic properties of compound **8** show that it can be absorbed low into the central nervous system with a BBB penetration value of 0.014. This could mean that it does not affect the functioning of the central nervous system. It is also predicted that compound binds strongly to plasma proteins with the PPP penetration value of 100. This value can indicate that the target compound's high binding level to plasma proteins can function as a drug depot or that it cannot even cross the membrane. Hence, the target compound has difficulty reaching the target protein. Plasma protein binding (PPP) is a bound fraction that is an indicator to measure the ability of a compound to diffuse to its molecular site of action. Drugs not strongly bound to plasma proteins are more likely to reach their target receptors and have positive pharmacological effects [37]. Its HIA value is in the range of 96.52%, which means that it has a good absorption profile. Caco-2 cell permeability, with a value of 16.401 nm/sec, shows that it can be absorbed well by the human intestine. Caco-2 cells are a human intestinal epithelial cancer cell line that mimics the

human intestinal epithelium, so the permeability of Caco-2 cells is usually used as a model to evaluate the permeability of new drug candidates in the intestine [38].

A toxicity prediction was carried out using the AdmetSAR online database. The results show that the compound 8 studied is non-carcinogenic. Furthermore, compound **8** does not irritate the skin, meaning that the compound does not cause allergic contact dermatitis. It should be noted that this compound is hepatotoxic. Drug-induced liver injury (DILI) is condition caused by certain medications that can damage the liver. DILI may be the result of direct toxicity from the administered drugs or their metabolites, or injury that results from immune-mediated mechanisms [39]. The hepatotoxicity of a drug can cause death and inflammation of hepatocyte cells [40]. Therefore, DILI is the main assessment for the rejection or withdrawal of drugs from the market in the pharmaceutical industry [41].

4. CONCLUSIONS

A novel benzensulphonylurea substituted pyridazinone derivative compound, namely the compound (E)-N'-(1-(4-(3-(4-methoxyphenyl)-6-oxopyridazine-1 (6H)-yl)phenyl)ethylidene)-4-methylbenzenesulphonohydrazide (**8)** has been successfully synthesized through three reaction stages. The suitability of the synthesized structure was confirmed using IR spectroscopy, ^{1}H-NMR, ^{13}C-NMR, and HRMS. The results of the molecular docking study showed that the compound **8** is predicted as a PPAR-γ agonist, so it can be developed as a candidate antidiabetic therapeutic agent to increase insulin sensitivity. Further research, such as in vitro and in vivo tests, is needed to obtain valid information. Furthermore, the ADMET profile shows that compound **8** has moderate ADME properties. However, it is hepatotoxic. Modifying the structure of compound **8** needs to be considered for its safety as a candidate antidiabetic therapeutic agent.

ACKNOWLEDGMENTS

The researchers would like to thank the researchers for the DIPA BLU research fund-ing assistance Number SP DIPA-025.04.2.424157/2022. Institute for Research and Community Service, UIN Sultan Syarif Kasim Riau.

REFERENCES

1. IDF Diabetes Atlas. *International Diabetes Federation*. Vol 102.; 2021. doi:10.1016/j.diabres.2021.10.013
2. Abuelizz HA, Iwana NANI, Ahmad R, Anouar EH, Marzouk M, Al-Salahi R. Synthesis, biological activity and molecular docking of new tricyclic series as α-glucosidase inhibitors. *BMC Chem*. 2019;13(3):1-14. doi:10.1186/s13065-019-0560-4
3. Keri RS, Patil MR, Patil SA, Budagupi S. A comprehensive review in current developments of benzothiazole-based molecules in medicinal chemistry. *Eur J Med Chem*. 2015;89:207-251. doi:10.1016/j.ejmech.2014.10.059
4. Janani C, Ranjitha Kumari BD. PPAR gamma gene - A review. *Diabetes Metab Syndr Clin Res Rev*. 2015;9(1):46-50. doi:10.1016/j.dsx.2014.09.015
5. Milligan G, Shimpukade B, Ulven T, Hudson BD. Complex pharmacology of free fatty acid receptors. *Chem Rev*. 2017;117(1):67-110. doi:10.1021/acs.chemrev.6b00056
6. Belete TM. A recent achievement in the discovery and development of novel targets for the treatment of type-2 diabetes mellitus. *J Exp Pharmacol*. 2020;12:1-15. doi:10.2147/JEP.S226113
7. Choi SS, Park J, Choi JH. Revisiting PPARγ as a target for the treatment of metabolic disorders. *BMB Rep*. 2014;47(11):599-608. doi:10.5483/BMBRep.2014.47.11.174
8. Park KS, Choi SH, Chung SS. Re-highlighting the action of PPARγ in treating metabolic diseases [version 1; referees: 2 approved]. *F1000Research*. 2018;7:1-9. doi:10.12688/f1000research.14136.1
9. Steven E. Nissen, M.D., and Kathy Wolski MPH. Effect of Rosiglitazone on the Risk of Myocardial Infarction and Death from Cardiovascular Causes. *N Engl J Med*. 2007;356(24). doi:10.1056/NEJMoa072761
10. Julie NL, Julie IM, Kende AI, Wilson GL. Mitochondrial dysfunction and delayed hepatotoxicity: Another lesson from troglitazone. *Diabetologia*. 2008;51(11):2108-2116. doi:10.1007/s00125-008-1133-6
11. Wu D, Eeda V, Undi RB, et al. A novel peroxisome proliferator-activated receptor gamma ligand improves insulin sensitivity and promotes browning of white adipose tissue in obese mice. *Mol Metab*. 2021;54(October):101363. doi:10.1016/j.molmet.2021.101363
12. Mourad AAE, Mourad MAE. Enhancing insulin sensitivity by dual PPARγ partial agonist, β-catenin inhibitor: Design, synthesis of new αphthalimido-o-toluoyl2-aminothiazole hybrids. *Life Sci*. 2020;259(June):118270. doi:10.1016/j.lfs.2020.118270
13. Jyoti Singh DS, Bansal & R. Pyridazinone: an attractive lead for anti- inflammatory and analgesic drug discovery. *Future Med Chem*.

2017;9(1):95-127. doi:10.2307/j.ctvnwc0d0.18

14. Khokra SL, Khan SA, Thakur P, Chowdhary D, Ahmad A, Husain A. Synthesis, Molecular Docking and Potential Antioxidant Activity of Di/Trisubstituted Pyridazinone Derivatives. *J Chinese Chem Soc*. 2016;63(9):739-750. doi:10.1002/jccs.201600051
15. Ahmed EM, Kassab AE, El-Malah AA, Hassan MSA. Synthesis and biological evaluation of pyridazinone derivatives as selective COX-2 inhibitors and potential anti-inflammatory agents. *Eur J Med Chem*. 2019;171:25-37. doi:10.1016/j.ejmech.2019.03.036
16. Khan A, Diwan A, Thabet HK, Imran M. Synthesis of novel N-substitutedphenyl-6-oxo-3-phenylpyridazine derivatives as cyclooxygenase-2 inhibitors. *Drug Dev Res*. 2020;81(5):573-584. doi:10.1002/ddr.21655
17. Nagle P, Pawar Y, Sonawane A, Bhosale S, More D. Docking simulation, synthesis and biological evaluation of novel pyridazinone containing thymol as potential antimicrobial agents. *Med Chem Res*. 2014;23(2):918-926. doi:10.1007/s00044-013-0685-2
18. Dundar Y, Kuyrukcu O, Eren G, Senol Deniz FS, Onkol T, Orhan IE. Novel pyridazinone derivatives as butyrylcholinesterase inhibitors. *Bioorg Chem*. 2019;92(September). doi:10.1016/j.bioorg.2019.103304
19. Yaseen R, Pushpalatha H, Reddy GB, et al. Design and synthesis of pyridazinone-substituted benzenesulphonylurea derivatives as anti-hyperglycaemic agents and inhibitors of aldose reductase – an enzyme embroiled in diabetic complications. *J Enzyme Inhib Med Chem*. 2016;31(6):1415-1427. doi:10.3109/14756366.2016.1142986
20. Firoozpour L, Kazemzadeh Arasi F, Toolabi M, et al. Design, synthesis and α-glucosidase inhibition study of novel pyridazin-based derivatives. *Med Chem Res*. 2023;32(4):713-722. doi:10.1007/s00044-023-03027-9
21. Chaudhry F, Ather AQ, Akhtar MJ, et al. Green synthesis, inhibition studies of yeast α-glucosidase and molecular docking of pyrazolylpyridazine amines. *Bioorg Chem*. 2017;71:170-180. doi:10.1016/j.bioorg.2017.02.003
22. Loghman Firoozpour, Setareh Moghimi, Somayeh Salarinejad, Mahsa Toolabi, Mahdi Rafsanjani, Roya Pakrad, Farzaneh Salmani, Seyed Mohammad Shokrolahi, Seyed Esmail Sadat Ebrahimi SK and AF. Synthesis, α-Glucosidase inhibitory activity and docking studies of Novel Ethyl 1,2,3-triazol-4-ylmethylthio-5,6-diphenylpyridazine-4-carboxylate derivatives. *BMC Chem*. 2023;17(1):4-13. doi:10.1186/s13065-023-00973-8
23. Akdağ M, Özçelik AB, Demir Y, Beydemir Ş. Design, synthesis, and aldose reductase inhibitory effect of some novel carboxylic acid derivatives bearing 2-substituted-6-aryloxo-pyridazinone moiety. *J Mol Struct*. 2022;1258:132675. doi:https://doi.org/10.1016/j.molstruc.2022.132675
24. Zaoui Y, Ramli Y, Tan SL, et al. Synthesis, structural characterisation and theoretical studies of a novel pyridazine derivative: Investigations of anti-inflammatory activity and inhibition of α-glucosidase. *J Mol Struct*. 2021;1234:130177. doi:10.1016/j.molstruc.2021.130177
25. Moghimi S, Toolabi M, Salarinejad S, et al. Design and synthesis of novel pyridazine N-aryl acetamides: In-vitro evaluation of α-glucosidase inhibition, docking, and kinetic studies. *Bioorg Chem*. 2020;102(June):104071. doi:10.1016/j.bioorg.2020.104071
26. Kharbanda C, Alam MS, Hamid H, et al. Antidiabetic effect of novel benzenesulfonylureas as PPAR-γ agonists and their anticancer effect. *Bioorganic Med Chem Lett*. 2015;25(20):4601-4605. doi:10.1016/j.bmcl.2015.08.062
27. Cruz S, Cifuentes D, Hurtado N, Román M. Síntesis de piridazin-3(2H)-onas asistida por microondas en condiciones libre de disolvente. *Inf Tecnol*. 2016;27(5):57-62. doi:10.4067/S0718-07642016000500007
28. Allam HA, Kamel AA, El-Daly M, George RF. Synthesis and vasodilator activity of some pyridazin-3(2H)-one based compounds. *Future Med Chem*. 2020;12(1):37-50. doi:10.4155/fmc-2019-0160
29. Tiryaki D, Sukuroglu M, Dogruer DS, Akkol E, Ozgen S, Sahin MF. Synthesis of some new 2,6-disubstituted-3(2H)-pyridazinone derivatives and investigation of their analgesic, anti-inflammatory and antimicrobial activities. *Med Chem Res*. 2013;22(6):2553-2560. doi:10.1007/s00044-012-0253-1
30. Özdemir Z, Alagöz MA, Akdemir AG, Özçelik AB, Özçelik B, Uysal M. Studies on a novel series of 3(2H)-pyridazinones: Synthesis, molecular modelling, antimicrobial activity. *J Res Pharm*. 2019;23(5):960-972. doi:10.35333/jrp.2019.43
31. Rahim F, Zaman K, Taha M, et al. Synthesis, in vitro alpha-glucosidase inhibitory potential of benzimidazole bearing bis-Schiff bases and

their molecular docking study. *Bioorg Chem*. 2020;94:103394. doi:10.1016/j.bioorg.2019.103394

32. Shi GQ, Dropinski JF, McKeever BM, et al. Design and synthesis of α-aryloxyphenylacetic acid derivatives: A novel class of PPARα/γ dual agonists with potent antihyperglycemic and lipid modulating activity. *J Med Chem*. 2005;48(13):4457-4468. doi:10.1021/jm0502135
33. Mackerell AD, Banavali N, Foloppe N. <MacKerellBiopolymer2001.pdf>. Published online 2001:257-265.
34. Jász Á, Rák Á, Ladjánszki I, Cserey G. Optimized GPU implementation of Merck Molecular Force Field and Universal Force Field. *J Mol Struct*. 2019;1188:227-233. doi:10.1016/j.molstruc.2019.04.007
35. Nazreen S, Alam MS, Hamid H, et al. Thiazolidine-2,4-diones derivatives as PPAR-γ agonists: Synthesis, molecular docking, in vitro and in vivo antidiabetic activity with hepatotoxicity risk evaluation and effect on PPAR-γ gene expression. *Bioorganic Med Chem Lett*. 2014;24(14):3034-3042. doi:10.1016/j.bmcl.2014.05.034
36. Lipinski CA. Rule of five in 2015 and beyond: Target and ligand structural limitations, ligand chemistry structure and drug discovery project decisions. *Adv Drug Deliv Rev*. 2016;101:34-41. doi:10.1016/j.addr.2016.04.029
37. Singh SK, Valicherla GR, Bikkasani AK, et al. Elucidation of plasma protein binding, blood partitioning, permeability, CYP phenotyping and CYP inhibition studies of Withanone using validated UPLC method: An active constituent of neuroprotective herb Ashwagandha. *J Ethnopharmacol*. 2021;270(2021):1-25. doi:10.1016/j.jep.2021.113819
38. Van Breemen RB, Li Y. Caco-2 cell permeability assays to measure drug absorption. *Expert Opin Drug Metab Toxicol*. 2005;1(2):175-185. doi:https://doi.org/10.1517/17425255.1.2.175
39. Stefan David and James P Hamilton. Drug-induced liver injury. *US Gastroenterol Hepatol Rev*. 2010;1(6):73-80. https://europepmc.org/article/pmc/3160634
40. Andrea Iorga LD and NK. Drug-Induced Liver Injury: Cascade of Events Leading to Cell Death, Apoptosis or Necrosis. *Int J Mol Sci*. 2017;18(1018):1-25. doi:https://doi.org/10.3390/ijms18051018
41. Jiang J, Pieterman CD, Ertaylan G, Peeters RLM, de Kok TMCM. *The Application of Omics-Based Human Liver Platforms for Investigating the Mechanism of Drug-Induced Hepatotoxicity in Vitro*. Vol 93. Springer Berlin Heidelberg; 2019. doi:10.1007/s00204-019-02585-5